Chemistry in Stringland: One-Dimensional Complexes of Main-Group Metal Ions with the Ligands $NC_{2n}X$ (X = N, CH; n = 0, 1, 2, 3)

Simon Petrie*

Department of Chemistry, the Faculties, Australian National University, Canberra ACT 0200 Australia

Received: July 21, 2003; In Final Form: October 2, 2003

Complexation by M^+ (M = Li, Be, Na, Mg, Al, K, Ca) of the highly unsaturated linear molecules $NC_{2n}X$ (X = N, CH; n = 0, 1, 2, 3) occurs exclusively by σ coordination to the terminal N atom, yielding linear molecular cations that are here characterized using high-level, counterpoise-corrected ab initio calculations. We argue that these complexes, with a total absence of steric hindrance through nonbonding interactions, form an excellent "test set" for the purpose of investigating, in detail, the nature of the metal ion/ligand interaction. We analyze the influence of ionic, covalent, and repulsive energy contributions to the M^+/ligand interaction for these species, using two different energy-decomposition schemes, and present also a complementary interpretation using the atoms-in-molecules (AIM) approach. Differences between the $M^+-NC_{2n}X$ bond dissociation energies (BDEs) of the highly polar cyanopolyynes $HC_{2n+1}N$ versus the analogous nonpolar dicyanopolyynes $NC_{2n}N$ diminish as the intervening carbon chain length increases, indicating that the local bond polarity of the coordinating CN group dominates over the ligand's overall polarity (or lack thereof) as an influence of M^+/ligand bond strength. The cyanopolyyne and dicyanopolyyne adducts of alkaline earth ions Be^+, Mg^+, and Ca^+ and of Al^+, whereas largely ionic in character, also possess significant overlying covalent tendencies. In contrast, the adducts of alkali metal ions Li^+, Na^+, and K^+ can indeed be treated as essentially purely ionic. Among the results reported here, one striking observation (for which an underlying physical basis remains elusive) is that the $M^+-NC_{2n}X$ series featuring an alkali metal ion exhibits a remarkably close adherence to the r^{-12} dependence of the empirically assigned repulsive potential energy term in the (12, 6) Lennard-Jones potential.

1. Introduction

Several recent mass spectrometric and computational studies[1−15] have highlighted the importance of metal ion/nitrogen-bearing ligand interactions within biochemical systems. In many of the main-group metal ion complexes of this type that have been recently studied, σ coordination to the N atom's lone pair is found to augment or to outweigh the strength of possible cation/π interactions.[1−5,7−10,12,14] To understand this biochemically important class of metal ion/nitrogenated ligand interactions better, there is a clear need for a reliable measure of the metal ion/ligand bond dissociation energy (BDE) within a wide range of σ-coordinated complexes[11,15,16] as well as an exploration of the underlying factors that contribute to this mode of complexation. Here, we suggest that the $M^+/NC_{2n}X$ complexes (M = Li, Be, Na, Mg, Al, K, Ca; n = 0, 1, 2, 3; X = N, CH) constitute an excellent system for investigating the metal ion/nitrogen bond.

The cyanopolyynes, $NC_{2n}CH$, and dicyanopolyynes, $NC_{2n}N$, have no known biochemical relevance. Nevertheless, these linear compounds have several attractive features for researchers as well as for metal ions. The cyanopolyynes are highly polar molecules, but the dicyanopolyynes lack a permanent electric dipole moment. In both sets of ligands, σ coordination to the terminal N atoms occurs on the molecular axis along which their permanent dipole moment (if nonzero) and polarizability are also maximized. Linear coordination to a metal ion M^+ also ensures that any steric influence on the strength of the M^+/ligand bond is minimized. The complete lack of steric hindrance, within a structurally consistent family of ligands in which both nonpolar and highly polar examples follow a regular size distribution, greatly assists the exploration of several key factors that impinge, in the most general sense, on metal ion complexation.

Many previous experimental and theoretical studies have dealt with the coordination of main-group metal ions to N_2.[17−32] Several studies have also featured the M^+/HCN complexes.[24,33−36] A distinct preference for the end-on coordination of M^+ is consistently seen for both of these ligands. Investigations of main-group metal ion coordination to the larger homologues have been restricted to theoretical studies of the reactions of Na^+, Mg^+, and Al^+ with $HC_{2n+1}N$,[37−39] processes implicated in the formation of several observed metal cyanides[40−44] in outflowing circumstellar envelopes and protoplanetary nebulae. Very recently, we have reported[45] thermochemical, structural, and spectroscopic parameters relevant to the complexation of Ca^+ by $HC_{2n+1}N$, a process potentially capable of producing a further, as yet unseen, metal cyanide CaNC under conditions appropriate to the astrophysical environments populated by those metal cyanides seen to date. No prior investigations of the other metal ions with the cyanopolyynes nor of any metal ions with any of the dicyanopolyynes $NC_{2n}N$ (n = 1, 2, 3 ...) have yet been undertaken. In the present work, we use quantum chemical techniques that have been specifically tailored to deliver high-quality thermochemical parameters for metal ion/ligand complexes[46−48] to study the interactions between main-group metal ions and the identified series of polyynic N-terminated ligands.

* E-mail: simon.petrie@anu.edu.au.

10.1021/jp0361226 CCC: $25.00
Published on Web 11/11/2003

2. Theoretical Methods

Geometry optimization and vibrational frequency calculations used the hybrid density functional B3-LYP (featuring Becke's three-parameter nonlocal exchange functional[49] and the correlation functional of Lee, Yang, and Parr)[50] with the triple-split-valence 6-311+G** basis set. Single-point total energy calculations employing the B3-LYP/6-311+G** optimized geometries were performed to yield total energies according to various "model chemistry" approaches within the widely used Gaussian-2 (G2) family[51,52] of computational techniques. Although a detailed description of the G2 methodology has been presented previously,[51] an outline here may assist in delineating the variants employed in the present work. The standard prescription for total energy obtained using the G2 procedure is[51]

$$E_0(\mathrm{G2}) = [\mathrm{QCISD(T)/B1G} + \mathrm{MP2/B1G} - \mathrm{MP4/B1G}] + [\mathrm{MP4/B2G} - \mathrm{MP2/B2G}] + [\mathrm{MP4/B3G} - \mathrm{MP2/B3G}] + \mathrm{MP2/B4G} + \mathrm{ZPE} + \mathrm{HLC} \quad (1)$$

and the corresponding prescription for the less computationally expensive G2(MP2) procedure is[53]

$$E_0(\mathrm{G2(MP2)}) = [\mathrm{QCISD(T)/B1G} - \mathrm{MP2/B1G}] + \mathrm{MP2/B4G} + \mathrm{ZPE} + \mathrm{HLC} \quad (2)$$

where the constituent levels of theory are second- (MP2) and fourth-order (MP4) Møller−Plesset perturbation theory and quadratic configuration interaction with the inclusion of single, double, and perturbative triplet excitations (QCISD(T)). The Gaussian basis sets B*i*G ($i = 1-4$) are respectively 6-311G**, 6-311+G**, 6-311+G(2df,p), and 6-311+G(3df,2p). ZPE denotes the inclusion of the calculated zero-point vibrational energy, and HLC (higher-level correction) seeks to remedy various deficiencies associated with basis set incompleteness, with the failure of the "additivity approximation,"[51,54] or inherent within the highest level of theory (QCISD(T)) employed within the G2 or G2(MP2) method.

Throughout, we have used B3-LYP/6-311+G** optimized geometries and zero-point vibrational energies in place of the MP2/6-31G* and HF/6-31G* values for these parameters prescribed in the standard Gaussian methods.[51] Calculations used in the present work additionally differ from standard G2 or G2(MP2) as follows. In all determinations of the M^+/ligand bond dissociation energy (BDE), a counterpoise correction (CP) for basis set superposition error (BSSE) has been applied according to the method of Boys and Bernardi[55] and using the MP2/B4G level of theory. The inclusion of this CP term yields significantly better agreement with high-precision laboratory BDE values for complexes including Na^+ [47,56] or other main-group metal ions.[48,56] For species containing Li^+, Na^+, Mg^+, or Al^+, the "inner-valence" 1s (Li) or 2s, 2p (Na, Mg, Al) orbitals are included within the correlation space in all single-point total-energy calculations.[46,57−59] In keeping with usage in previous studies,[46−48,60] we denote such departures from the standard frozen-core assignment as a 'thawed' correlation space (e.g., G2thaw or MP2thaw). The additional difference from standard Gaussian methods, in the calculations featuring Na^+, Mg^+, or Al^+, is the use of "partially decontracted" B4G metal-atom basis sets that we have described in previous studies.[47,48] This use of a nonstandard metal ion basis set, justified by its delivery of much lower metal ion terms in counterpoise correction calculations for BSSE,[47,48] is denoted by a d prefix as in dG2thaw.

TABLE 1: Counterpoise-Corrected M^+/Ligand Bond-Dissociation Energy (BDE) Values for Dinitrogen, Dicyanopolyynes, and Cyanopolyynes

	BDE (kJ mol^{-1})[a]							
		dicyanopolyynes			cyanopolyynes			
M^+	N_2	NCCN	NC_4N	NC_6N[b]	HCN	HC_3N	HC_5N[c]	HC_7N[c]
Li^+[d]	47.2	102.8	127.3	142.2	140.7	155.3	165.4	174.5
[e]	**47.8**	**102.8**	**126.4**		**141.4**	**155.1**	**163.8**	
Be^+[f]	81.4	197.8	245.8	261.6	246.6	281.0	305.5	320.6
[g]	**86.6**	**202.1**	**248.4**		**251.1**	**285.7**	**306.9**	
Na^+[f]	28.6	68.9	87.6	98.4	101.9	112.4	119.5	121.9
[h]	**28.9**	**68.8**	**86.9**[i]		**102.3**	**112.3**	**118.2**[i]	
Mg^+[f]	25.9	88.2	117.5	119.1	128.3	147.4	161.2	165.8
[h]	**26.5**	**88.7**	**118.0**[i]		**129.4**	**148.4**	**160.6**[i]	
Al^+[f]	19.4	68.8	97.9	117.3	106.5	128.0	143.6	153.5
[h]	**18.5**	**67.4**	**96.1**[i]		**106.7**	**127.3**	**141.2**[i]	
K^+[j]	18.5	48.5	63.6	72.9	76.6	85.3	91.3	94.4
[g]	**17.9**	**47.1**	**61.9**[k]		**75.7**	**83.7**	**89.1**[k]	
Ca^+[j]	18.0	69.4	93.7[l]		104.8[m]	120.8[m]	131.9[m]	137.3[m]
[g]	**17.7**	**68.1**	**91.8**[k,l]		**104.1**[m]	**119.3**[m]	**128.9**[k,m]	

[a] Values shown are obtained from the CP-MP2/6-311+G(3df,2p) level of theory (normal font) or from the identified G2-based level of theory (bold font). Correlation spaces used in the calculations are specified. In all cases, optimized geometries employed are those obtained at the B3-LYP/6-311+G** level of theory. [b] Determined using counterpoise correction terms obtained for M^+/NC_4N, unless otherwise indicated. [c] Determined using counterpoise correction terms obtained for M^+/HC_3N. [d] All M^+ atomic orbitals (AOs) included in correlation space. [e] CP-G2(thaw) calculation. [f] M^+ 1s AO excluded from correlation space. [g] CP-G2 calculation, unless otherwise indicated. [h] CP-dG2thaw calculation, unless otherwise indicated. [i] CP-dG2(MP2)thaw calculation. [j] M^+ 1s, 2s, and 2p AOs excluded from correlation space. [k] CP-G2(MP2) calculation. [l] Determined using counterpoise correction terms obtained for M^+/NCCN. [m] Previously reported in ref 66.

For metal ion complexes of ligands NC_6N and HC_7N, full G2- or G2(MP2)-based treatments were too unwieldy to pursue on the available computational platforms. Consequently, for these larger species, our ab initio exploration has been restricted to CP-corrected MP2/B4G calculations (where the B4G basis set and the correlation space employed are as defined above). Calculations at this level of theory were also executed as a matter of course as a component of the Gaussian-method variants for the smaller complexes.

The ab initio calculations described above were performed using the Gaussian 98 quantum chemistry program suite.[61] In supplementary calculations employing density functional theory (DFT) method B-LYP,[50,62] the Amsterdam density functional (ADF) package[63] was used for the exploration of bonding parameters within a selection of the target complexes.

3.Results and Discussion

3.1. Initial Overview of BDE Results. Our calculated BDE values, from the Gaussian-variant calculations and from single-point MP2 calculations, are summarized in Table 1. It is very gratifying to note that the MP2- and the G2-based calculations, both of which are counterpoise-corrected, show consistently good agreement, with BDE(Be^+-N_2) the only instance where the much more economical MP2 approach yields a value for which the variance from the Gaussian-based approach exceeds ±5 kJ mol^{-1}. Indeed, the calculations involving Be^+ (for which MP2 consistently underestimates the supposedly more reliable

TABLE 2: Calculated Electrostatic Parameters for Ligands Obtained at the B3-LYP/6-311+G Level of Theory**

		Q^b			α^c		
ligand	μ^a	*xx*	*yy*	*zz*	*xx*	*yy*	*zz*
N_2	0	−10.3182	−10.3182	−12.0196	7.829	7.829	15.325
NCCN	0	−21.1003	−21.1003	−30.5170	16.800	16.800	56.072
NC_4N	0	−32.0862	−32.0862	−51.4361	24.467	24.467	128.765
NC_6N	0	−43.0951	−43.0951	−74.5110	32.212	32.212	239.073
HCN	3.0568	−11.8392	−11.8392	−9.9550	10.441	10.441	22.577
HC_3N	3.9211	−22.9215	−22.9215	−21.2923	18.989	18.845	72.228
HC_5N	4.7026	−33.9643	−33.9643	−33.6208	26.778	26.773	153.918
HC_7N	5.4111	−45.0097	−45.0097	−46.5634	34.581	34.583	275.846

[a] Dipole moment (D). [b] Quadrupole moment (D Å). [c] Polarizability (au^3).

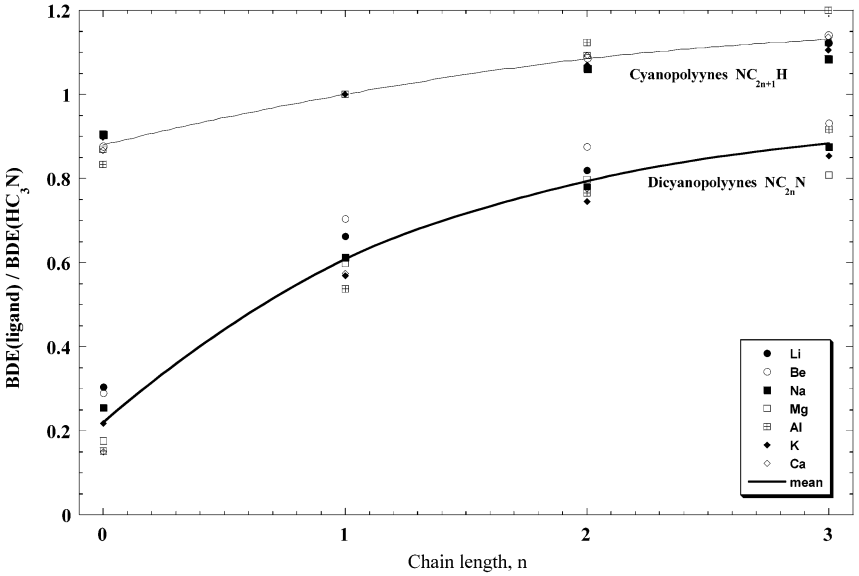

Figure 1. Dependence of M^+/ligand BDE on chain length *n*, normalized (for each metal ion) to BDE(M^+-NC_3H).

G2-based value by a few kJ mol^{-1}) are the only instances in Table 1 where the discrepancy between the two methods exceeds ±3 kJ mol^{-1}. This generally very close accord affords considerable confidence in the M^+/NC_6N and M^+/HC_7N BDEs for which calculation using MP2 theory is the only feasible option with the computational platform used in this study. We have noted[47] that CP-dG2thaw calculations on Na^+-containing adduct ions consistently yield BDE values that exceed the high-precision laboratory gas-phase sodium cation affinity values of McMahon and Ohanessian[64,65] by an increment of 2.8 ± 1.3 kJ mol^{-1}, and we surmise that the accuracy of the present counterpoise-corrected, G2-based calculations should similarly be competitive with the precision afforded by state-of-the-art laboratory practice in metal ion thermochemistry.

There are several trends evident in these BDEs. For a given metal ion, the M^+/cyanopolyyne BDE value clearly increases with increasing carbon chain length. This property, which has been previously noted in calculations on Na^+, Mg^+, and Al^+ complexes of cyanopolyynes,[39] is consistent with expectations regarding the increase in both ion/dipole attraction and ion/induced dipole attraction with increasing molecular size. For convenience, calculated electrostatic properties of the ligands are displayed in Table 2. In the absence of a permanent electric dipole moment, the dicyanopolyynes (among which we might also seek to include N_2 as the smallest member) also show an increase in BDE for a given metal ion with increasing ligand chain length. This can be understood in terms of ion/quadrupole and ion/induced dipole attractive interactions, of which the latter, dependent on the ligand's polarizability, appears more useful in understanding the general trend in BDEs for two reasons. First, there is a reasonably close correspondence between (both axial and perpendicular components of) the polarizabilities of $HC_{2n+1}N$ and $NC_{2n}N$ for a given value of *n*, in keeping with the apparent tendency for M^+/ligand BDEs (for a given M^+) to converge as *n* is increased (Figure 1). Second, attempts to optimize $M^+/NC_{2n}N$ complexes having C_{2v} symmetry, in which the point of coordination is defined as the NC_n-C_nN bond midpoint, have consistently revealed that these complexes show a major preference for end-on σ coordination, suggesting that the influence of the (highly directional) polarizability of the larger dicyanopolyynes substantially exceeds that of the (weakly directional) quadrupole moment. A more detailed discussion of the effects due to multipole moments and polarizabilities may be of limited value because it is arguably more appropriate to consider the influence of bond polarity (as explored through, for example, a "distributed multipoles" approach) rather than the influence of overall molecular properties. One possible indication of the role of bond polarity is that BDEs for NCCN (which is nonpolar overall but with highly polar C−N bonds) always exceed those for N_2 by more than 100%, whereas the corresponding increase in BDE in going from HCN to HC_3N is never more than about 20%. This inferred influence of *local* polarity may also help to explain the general tendency toward the convergence of dicyanopolyyne versus cyanopolyyne BDE values as the chain length increases (Figure 1): the more remote the ligand's further terminus, the less significant its identity as a CCH versus a CN moiety.

There is also a very obvious trend, for a given ligand, in BDE values for the various metals. The BDE(M^+-ligand) values in Table 1 diminish in the order $Be^+ > Li^+ > Mg^+ > (Na^+, Al^+,$

Ca^+) > K^+, except that BDE(M^+-N_2) is larger for Na^+ than for Mg^+. Implicit within this overall ranking, and entirely consistent with many previous experimental and theoretical studies of BDE values for main-group metal ions with simple ligands, is the tendency for BDE values to decrease with increasing row number for both the alkali metal ion and alkaline earth ion groups. This is explicable in terms of the supposed essentially ionic character of these complexes, with the lightest metal ions within a given group naturally exerting the greatest attraction for ligands by virtue of their small ionic radius. Nevertheless, a simple "hard-sphere" ion/neutral interaction cannot explain all of the BDE values. For example, Na^+ has the third highest BDE for N_2 but the second lowest BDE for most of the other ligands. This degree of inconsistency in the BDE rankings is at odds with a purely electrostatic model in which the only features of the ion are its charge and its effective radius. A deeper analysis of the bonding properties within these complexes may improve our understanding of their internal structure.

3.2. Extraction of Attractive and Repulsive Terms from the BDE Values. Dunbar[66] has described a decomposition of the metal ion/ligand bond dissociation energies into ionic, orbital, and repulsive terms. We may express this deconstruction as

$$\mathrm{BDE}(M^+-X) = -(\Delta E_{\mathrm{ionic}} + \Delta E_{\mathrm{orbital}} + \Delta E_{\mathrm{repuls}}) \quad (3)$$

where the attractive terms $\Delta E_{\mathrm{ionic}}$ and $\Delta E_{\mathrm{orbital}}$ denote the stabilization of the complex due, respectively, to the interaction of the metal ion's charge with the ligand's electrostatic potential field augmented by ion-induced polarization of the ligand and to the (nominally covalent) electronic orbital interactions associated with complexation, where $\Delta E_{\mathrm{repuls}}$ is the short-range repulsion energy that acknowledges the metal ion to be of finite size rather than a point charge. Within our ab initio calculations of BDE for the various complexes, these energy terms are not directly separable. However, we can access $\Delta E_{\mathrm{ionic}}$ to tolerably high accuracy by performing calculations on a given complex in which the metal ion is replaced by a point charge at the same location. Such calculations, which neglect both the metal ion's size and its (occupied and virtual) orbitals, effectively omit the $\Delta E_{\mathrm{orbital}}$ and $\Delta E_{\mathrm{repuls}}$ terms and need no correction for BSSE because they involve no additional superposition of basis sets upon complexation of the point charge. We have been able, in this manner, to determine $\Delta E_{\mathrm{ionic}}$ for all of the $M^+/NC_{2n}N$ and $M^+/NC_{2n+1}H$ (n = 0, 1, 2) complexes using the G2(MP2) approach for the ligand, and the resulting values are listed in Table 3. The difference between these $\Delta E_{\mathrm{ionic}}$ values and the BDE determinations made using the corresponding G2(MP2)-based method for the true M^+/ligand complexes yields the difference energy (i.e., the sum $\Delta E_{\mathrm{orbital}} + \Delta E_{\mathrm{repuls}}$) effectively at the same level of theory. Can we then isolate $\Delta E_{\mathrm{orbital}}$ and $\Delta E_{\mathrm{repuls}}$ from within this difference energy?

In Figure 2, we present a log/log graph of the difference energy ($\Delta E_{\mathrm{orbital}} + \Delta E_{\mathrm{repuls}}$) versus r[M−N]. The dependence of the difference energy upon the metal/ligand bond length is clearly steepest for the alkali metal ions that, lacking accessible valence electrons, are expected to exhibit negligible covalency in their ligation. If we seek to interpret the observed difference-energy slopes for the alkali metal ions—Li^+ (−10.9), Na^+ (−12.8), and K^+ (−13.2)—as representative of the purely repulsive term $\Delta E_{\mathrm{repuls}}$, it is rather remarkable that the general form of the alkali metal ion data adheres so closely to the r^{-12} dependence of the standard Lennard-Jones potential. However, further calculations have led us to conclude that this close match with the repulsive Lennard-Jones term (for which the historical adoption of an r^{-12} dependence was predominantly a mathematical convenience) is essentially fortuitous.

The difference energy (Figure 2) depends less steeply on the metal ion/ligand separation for the alkaline earth monocations Be^+ (slope = −4.5), Mg^+ (−5.6), and Ca^+ (−4.1) and for Al^+ (−6.1) than for the alkali metal ions. Two likely contributing effects to this trend are that, first, metal ions with one or two valence electrons are less well viewed as hard spheres and so have greater compressibility, resulting in a "softer" $\Delta E_{\mathrm{repuls}}$ component than is indicated by the approximate r^{-12} dependence seen for the alkali metal ions; second, complexes of the alkaline earth ions and Al^+ are expected to have nonnegligible electron-sharing interactions ($\Delta E_{\mathrm{orbital}}$) by virtue of the unsatisfied valences of these metal ions. Some measure of the separate $\Delta E_{\mathrm{repuls}}$ and $\Delta E_{\mathrm{orbital}}$ terms can be obtained by assuming that the weakly bonded M^+/N_2 complexes remain purely electrostatic (i.e, $\Delta E_{\mathrm{orbital}} = 0$) for all metal/ligand separations and that the M^+/NX repulsive interaction is independent of the identity of ligand atoms beyond the coordinating N atom. The assumption that M^+/N_2 remains purely electrostatic even at close metal/ligand separations is likely not strictly valid; nevertheless, this approach offers at least a method of quantifying feasible lower limits to $\Delta E_{\mathrm{repuls}}$ and upper limits to $\Delta E_{\mathrm{orbital}}$. The values for these parameters listed in Table 3 result from the assumptions indicated above and use the difference-energy curves for M^+/N_2 obtained from G2(MP2) calculations of $\Delta E_{\mathrm{ionic}}$ and the counterpoise-corrected BDE as a function of r(M−N). It is striking that this method yields positive upper limits for $\Delta E_{\mathrm{orbital}}$ for all of the alkali metal ion complexes of the cyano- and dicyanopolyynes (implying that $\Delta E_{\mathrm{orbital}}$ for these species may be either positive or negative), whereas the upper limits for $\Delta E_{\mathrm{orbital}}$ for the other metal ions are consistently negative. We interpret these results as indicating that the alkali metal ion complexes may or may not possess some covalent character (chemical intuition would suggest that they do not), whereas the complexes of alkali metal ions and Al^+ *do* unambiguously possess such character. Covalent interactions appear to contribute at least 10 kJ mol^{-1} to the binding energies of most of the nonalkali metal ion complexes of cyanopolyynes and dicyanopolyynes, rising to at least 30 kJ mol^{-1} in the examples of Be^+ and Al^+ with HC_5N.

Although it is hazardous to interpret blithely the upper limits to $\Delta E_{\mathrm{orbital}}$ as a reliable representation of the covalency in each M^+/ligand complex, it remains readily apparent that the chief distinguishing feature between the alkali metal ions and the other ions is the remarkably consistent adherence of the former, but not the latter, to an r^{-12} dependence for the nonionic component of the bond dissociation energy as displayed in Figure 2. If we assume that, for the alkali metal ion complexes, $\Delta E_{\mathrm{orbital}}$ is indeed zero, then the approach adopted here (incorporating an r^{-12} dependence for $\Delta E_{\mathrm{repuls}}$) might permit the computation of nonbonding repulsive (i.e., steric) energy terms in the BDEs for Na^+ and K^+ coordinated to 2D or 3D nitrogen-bearing ligands. In such ligands, those atoms not directly coordinated to M^+ are not completely in the N atom's "shadow," so we may well expect to see an essentially steric component in the BDE summation:

$$\mathrm{BDE}(M^+-X) = -(\Delta E_{\mathrm{ionic}} + \Delta E_{\mathrm{orbital}} + \Delta E_{\mathrm{repuls}} + \Delta E_{\mathrm{steric}}) \quad (4)$$

3.3. Atoms-in-Molecules Appraisal of the Metal/Ligand Bonding. The atoms-in-molecules (AIM) approach offers another means of discerning electrostatic or covalent interactions

TABLE 3: Ionic, Repulsive, and Orbital Components of the M^+/Ligand Bond-Dissociation Energy (BDE) Obtained from G2(MP2) Calculations Using a Point-Charge Model

		r(M−N)	BDE components/kJ mol^{-1} [a]				
M^+	ligand	Å	ΔE_{ionic}	$\Delta E_{repuls} + \Delta E_{orbital}$	ΔE_{repuls}	$\Delta E_{orbital}$	$-\Delta E_{total}$
Li^+	NN	2.061	−90.9	42.6	>42.6	<0	48.3
Li^+	NCCN	1.944	−187.0	84.2	>61	<23	102.8
Li^+	NCCCCN	1.906	−229.7	103.2	>69	<34	126.6
Li^+	NCH	1.927	−227.1	85.5	>64	<22	141.6
Li^+	NCCCH	1.895	−261.7	106.5	>72	<35	155.2
Li^+	NCCCCCH	1.876	−281.7	117.9	>77	<41	163.8
Be^+	NN	1.794	−140.0	52.4	>52.4	<0	87.6
Be^+	NCCN	1.654	−279.1	76.6	>91	<−14	202.5
Be^+	NCCCCN	1.617	−336.0	87.4	>106	<−18	248.6
Be^+	NCH	1.655	−317.1	65.3	>90	<−25	251.8
Be^+	NCCCH	1.613	−367.6	81.6	>108	<−26	286.0
Be^+	NCCCCCH	1.592	−396.3	89.5	>120	<−30	306.8
Na^+	NN	2.463	−50.1	21.0	>21.0	<0	29.1
Na^+	NCCN	2.334	−112.1	43.5	>31	<13	68.6
Na^+	NCCCCN	2.295	−140.8	53.9	>36	<18	86.9
Na^+	NCH	2.308	−149.0	46.8	>34	<13	102.2
Na^+	NCCCH	2.275	−170.3	58.0	>38	<20	112.3
Na^+	NCCCCCH	2.256	−182.8	64.6	>41	<24	118.2
Mg^+	NN	2.477	−49.2	21.6	>21.6	<0	27.5
Mg^+	NCCN	2.214	−130.4	41.0	>49	<−8	89.4
Mg^+	NCCCCN	2.151	−167.4	49.4	>58	<−9	118.0
Mg^+	NCH	2.188	−168.8	38.5	>52	<−13	130.3
Mg^+	NCCCH	2.134	−198.3	49.1	>62	<−13	149.2
Mg^+	NCCCCCH	2.104	−215.4	54.7	>69	<−14	160.6
Al^+	NN	2.855	−30.2	11.6	>11.6	<0	18.6
Al^+	NCCN	2.353	−109.5	42.2	>51	<−9	67.3
Al^+	NCCCCN	2.207	−156.1	60.0	>80	<−20	96.1
Al^+	NCH	2.291	−151.5	44.6	>62	<−17	107.0
Al^+	NCCCH	2.172	−190.1	62.7	>88	<−25	127.5
Al^+	NCCCCCH	2.107	−214.3	73.2	>106	<−33	141.2
K^+	NN	2.946	−27.1	8.9	>8.9	<0	18.2
K^+	NCCN	2.771	−67.8	20.5	>14	<7	47.3
K^+	NCCCCN	2.715	−88.9	27.0	>19	<8	61.9
K^+	NCH	2.722	−101.6	25.6	>18	<8	76.0
K^+	NCCCH	2.684	−114.5	30.4	>21	<9	84.1
K^+	NCCCCCH	2.662	−122.7	33.6	>24	<10	89.1
Ca^+	NN	2.690	−37.0	19.0	>19.0	<0	18.0
Ca^+	NCCN	2.475	−94.4	26.2	>34	<−8	68.2
Ca^+	NCCCCN	2.419	−121.7	29.9	>43	<−13	91.8
Ca^+	NCH	2.448	−129.7	25.3	>39	<−14	104.4
Ca^+	NCCCH	2.400	−149.4	29.9	>46	<−16	119.6
Ca^+	NCCCCCH	2.373	−161.3	32.5	>51	<−18	128.9

[a] Component energy terms are defined as and obtained in the manner specified in the text.

between adjacent atoms. We have performed an AIM study, at the B3-LYP/6-311+G** level of theory, of M^+ with N_2, with HCN, and with NCCN, with salient results summarized in Table 4. The AIM results of interest for each species include $\nabla^2\rho(r_c)$, the Laplacian of the electron density at the bond critical point r_c, q_{M^+}, the AIM formal charge on the metal atom, and $BO_{cov}(M^+-N)$, the AIM covalent bond order for the identified bond. It can be seen that the $\nabla^2\rho(r_c)$ value for each M^+ is always positive and is consistently larger for M^+ coordination to NCCN or HCN than to N_2. A positive $\nabla^2\rho(r_c)$ value indicates that the M^+/ligand interaction is dominated by ionic rather than covalent effects, although the magnitude of $\nabla^2\rho(r_c)$ is dependent on the intensity of the M^+/ligand interaction as well as on its (ionic or covalent) character. A largely ionic interaction between M^+ and the ligand is supported, in all cases, by the AIM metal-atom formal charge values q_{M^+}, which are invariably between 0.96 and 1.01. Nevertheless, indications of some covalent character are evident for the Be^+ complexes, which exhibit substantially the highest bond-critical-point density values among the species surveyed, and the Al^+ complexes for which the Laplacian values are much lower than those of the complexes of the corresponding alkali metal ion Na^+ despite comparatively large $\rho(r_c)$ values for Al^+/NCCN and Al^+/NCH. The Be^+/ligand and Al^+/NCR (R = H, CN) AIM covalent bond orders are also notably the largest seen among the complexes in Table 4, followed by the bond-order values determined for Mg^+ and Ca^+ with either NCCN or HCN. Finally, we can note also that the alkaline earth ion complexes invariably feature a significant excess of α spin over β spin contribution in the overall covalent bond order, indicating that radical stabilization through delocalization of the unpaired electron is an important factor in the drive toward partial covalent bond character in these odd-electron complex ions.

The AIM results confirm our inference (based on BDE decomposition) that the alkali metal ion complexes feature the smallest degree of covalent character and Be^+ and Al^+ exhibit the largest. Furthermore, the covalent bond orders invariably fall far short of unity (or even semiunity), thus supporting also our interpretation that even in the Be^+ and Al^+ complexes the contribution from electron sharing remains subservient to the stronger electrostatic interaction between M^+ and the ligand.

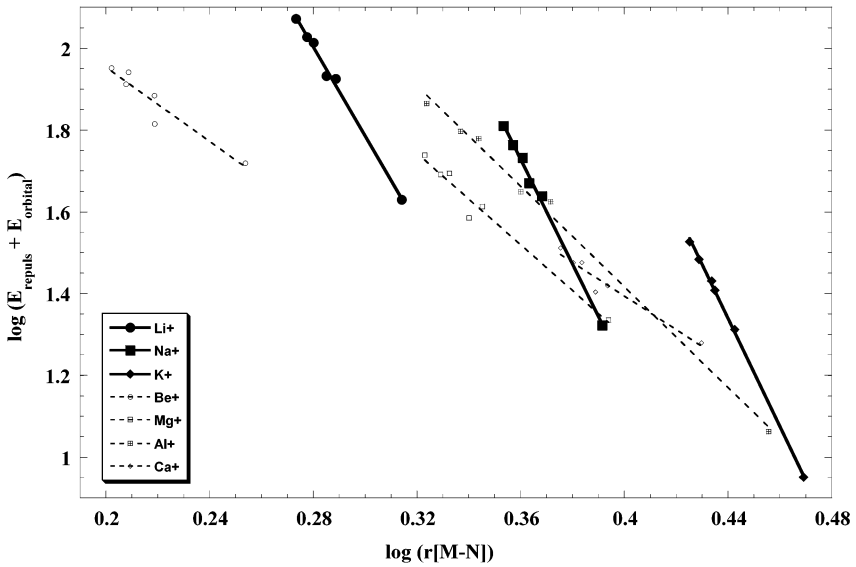

Figure 2. Dependence of the summed nonionic contributions to the overall M^+/ligand BDE, namely, $\Delta E_{orbital} + \Delta E_{repuls}$, on the optimized M^+-N internuclear separation. Plotted values, obtained from Table 3, were determined from total and ionic energies determined at the CP-dG2(MP2)thaw or CP-G2(MP2) level of theory.

TABLE 4: Summary of Results of an Atoms-in-Molecules (AIM) Analysis at the B3-LYP/6-311+G Level of Theory of the N_2, HCN, and NCCN Metal Ion Adducts**

M^+	ligand	$\rho(r_c)$ [a]	$\nabla^2\rho(r_c)$ [b]	$r(M^+-N)$/Å [c]	$r(M^+-r_c)$/Å [d]	$r(r_c-N)$/Å [d]	q_M+ [e]	$BO_{cov}(M^+-N)$ [f]	$BO_\alpha(M^+-N)$ [g]
Li^+	NN	0.0222	0.1440	2.061	1.299	0.761	0.974	0.068	
Li^+	NCCN	0.0315	0.2120	1.944	1.225	0.719	0.963	0.095	
Li^+	NCH	0.0333	0.2239	1.927	1.214	0.713	0.962	0.101	
Be^+	NN	0.0506	0.2673	1.794	1.189	0.605	0.988	0.291	0.205
Be^+	NCCN	0.0762	0.4183	1.654	1.087	0.567	0.966	0.352	0.240
Be^+	NCH	0.0768	0.4138	1.655	1.087	0.567	0.967	0.354	0.240
Na^+	NN	0.0153	0.0904	2.463	1.373	1.090	0.978	0.073	
Na^+	NCCN	0.0219	0.1349	2.334	1.298	1.036	0.967	0.105	
Na^+	NCH	0.0237	0.1464	2.308	1.283	1.024	0.964	0.114	
Mg^+	NN	0.0170	0.0628	2.477	1.431	1.045	1.006	0.191	0.136
Mg^+	NCCN	0.0292	0.1667	2.214	1.275	0.939	0.984	0.255	0.167
Mg^+	NCH	0.0310	0.1835	2.188	1.259	0.929	0.980	0.264	0.170
Al^+	NN	0.0148	0.0206	2.855	1.478	1.377	0.987	0.161	
Al^+	NCCN	0.0314	0.0417	2.353	1.360	0.993	0.971	0.324	
Al^+	NCH	0.0344	0.0597	2.291	1.338	0.954	0.968	0.348	
K^+	NN	0.0107	0.0466	2.946	1.472	1.474	0.986		
K^+	NCCN	0.0164	0.0739	2.771	1.382	1.389	0.976	0.108	
K^+	NCH	0.0186	0.0837	2.722	1.358	1.364	0.972	0.122	
Ca^+	NN	0.0171	0.0801	2.690	1.381	1.309	0.997	0.172	0.117
Ca^+	NCCN	0.0297	0.1435	2.475	1.259	1.216	0.975	0.254	0.162
Ca^+	NCH	0.0321	0.1536	2.448	1.245	1.204	0.970	0.270	0.170

[a] Energy density at the M^+-N bond critical point. [b] Laplacian of the energy density at the M^+-N bond critical point. [c] M^+-N internuclear separation in the optimized metal−ligand complex. [d] Separation of the bond critical point r_c from the indicated atom. [e] AIM formal charge on the metal atom. [f] Calculated covalent bond order of the M^+-N interaction. [g] Calculated α-spin contribution to the overall covalent bond order of the M^+-N interaction for the alkaline earth ion complexes.

3.4. Insights from the Morokuma/Ziegler Bond-Energy Decomposition Scheme. We have performed an alternative analysis of the M^+/ligand bond energy within these complexes using a decomposition scheme originally advanced by Morokuma[67,68] and Ziegler.[69,70] This scheme, as implemented[71,72] within the density functional theory program suite ADF,[63] involves the partitioning of energy terms

$$\Delta E_{bond} = \Delta E_{prep} + \Delta V_{elst} + \Delta E_{Pauli} + \Delta E_{oi} \qquad (5)$$

where the component terms are ΔE_{prep}, the energy required to deform the fragments (here M^+ and $NC_{2n}X$) from their separated equilibrium structures to the geometries adopted within the optimized complex; ΔV_{elst}, the classical electrostatic interaction between the fragments' intrinsic charge distributions; ΔE_{Pauli}, the Pauli repulsion representing the destabilizing interactions between occupied orbitals; and ΔE_{oi}, the (attractive) orbital interaction energy summing covalent and electron-transfer interactions. For the species under discussion here, ΔE_{oi} can also be usefully subdivided as $\Delta E_{oi}(\sigma) + \Delta E_{oi}(\pi)$. Results of this energy-decomposition approach are shown in Table 5.

The BDE values obtained at the B-LYP/TZP level of theory, shown in Table 5, systematically exceed the counterpoise-corrected values in Table 1. The discrepancy between the DFT values and the Table 1 values exceeds 20% in some instances, and the largest absolute difference (35 kJ mol^{-1}) is seen for

TABLE 5: Components of the M^+/Ligand Bond-Dissociation Energy (BDE) in kJ mol^{-1} Obtained from B-LYP/TZP Calculations According to the Morokuma/Ziegler Bond-Energy Decomposition Approach[67-70]

M^+	ligand	ΔE_{prep}[a]	ΔE_{Pauli}[a]	ΔV_{elst}[a]	$\Delta E_{oi}(\sigma)$[a]	$\Delta E_{oi}(\pi)$[a]	$-\Delta E_{total}$
Li^+	NCCN	−0.5	43.7	−79.2	−36.4	−46.4	118.8
Li^+	NCCCH	0.7	56.2	−137.6	−38.1	−55.6	174.3
Be^+	NCCN	1.1	414.8	−269.3	−245.3	−123.0	221.7
Be^+	NCCCH	2.8	463.7	−357.9	−270.1	−150.0	311.4
Na^+	NN	0.0	13.8	−22.9	−17.5	−11.7	38.2
Na^+	NCCN	−0.7	28.6	−60.8	−17.5	−27.5	77.8
Na^+	NC_4N	−0.6	34.6	−77.5	−17.8	−38.6	100.0
Na^+	NC_6N	0.5	38.2	−87.5	−18.2	−47.2	114.2
Na^+	NCH	0.2	34.6	−106.0	−18.0	−19.2	108.3
Na^+	NC_3H	0.9	38.9	−111.6	−17.6	−33.2	122.6
Na^+	NC_5H	0.4	41.8	−116.7	−17.8	−43.1	135.5
Na^+	NC_7H	0.6	44.5	−120.6	−18.1	−51.2	144.8
Mg^+	NN	0.2	79.8	−54.3	−44.6	−15.9	34.9
Mg^+	NCCN	−0.3	164.0	−137.5	−73.7	−49.0	96.5
Mg^+	NC_4N	0.0	194.0	−170.5	−83.9	−70.8	131.1
Mg^+	NC_6N	1.2	210.8	−189.3	-89.9	−87.1	154.3
Mg^+	NCH	0.4	176.4	−192.1	−82.0	−35.4	132.7
Mg^+	NC_3H	1.3	203.7	−212.2	−88.3	−62.9	158.4
Mg^+	NC_5H	1.3	219.1	−225.2	−93.0	−82.0	179.7
Mg^+	NC_7H	1.9	230.4	−234.2	−96.6	-96.8	195.3
Al^+	NN	0.1	40.9	−26.6	−27.4	−9.4	22.4
Al^+	NCCN	-0.3	167.7	−115.8	−80.5	−43.2	72.2
Al^+	NC_4N	-0.3	252.9	−173.2	−112.8	−74.7	108.0
Al^+	NC_6N	1.4	310.8	−211.4	−134.0	−100.5	133.7
Al^+	NCH	0.2	198.2	−175.2	−98.1	−33.3	108.2
Al^+	NC_3H	1.2	280.0	−222.2	−125.1	−69.8	135.8
Al^+	NC_5H	1.6	334.2	−254.3	−143.6	−98.4	160.5
Al^+	NC_7H	2.7	371.7	−276.4	−156.4	−120.9	179.3
K^+	NCCN	-0.4	25.9	−44.6	−13.2	−17.6	49.8
K^+	NCCCH	0.4	38.4	−89.1	−15.4	−22.5	88.2
Ca^+	NCCN	0.1	167.6	−134.9	−78.1	−40.5	85.8
Ca^+	NCCCH	0.7	204.1	−202.7	−90.6	−52.9	141.4

[a] Component energy terms are defined as and obtained in the manner specified in the text.

Mg^+/NC_6N. The divergence of the DFT and ab initio values arises, in part, through the lack of correction for either zero-point vibrational energy or basis set superposition error in the DFT values but may well represent additional inaccuracy of the DFT method used here. Note that because our primary intent with the DFT calculations is to explore trends in bonding influences and because the DFT calculations generally reproduce very well the BDE trends evident in Table 1, the apparent imprecision in individual B-LYP BDE values is not a cause for great concern. The ΔE_{prep} term is essentially negligible in all instances, exceeding only 1% of the DFT-determined bond dissociation energy in the instance of Al^+/NC_7H.

A comparison of the energy-term trends for the Na^+, Mg^+, and Al^+ complexes is informative. The alkali metal ion complexes are dominated by ΔV_{elst}; the N_2 complex is the only example for Na^+ where ΔE_{oi} exceeds ΔV_{elst} in magnitude. Separation of the ΔE_{oi} term into σ- and π-symmetry components reveals a remarkable consistency between $\Delta E_{oi}(\sigma)$ values for the eight Na^+ complexes, with all values lying between −17.4 and −18.3 kJ mol^{-1}. $\Delta E_{oi}(\pi)$, which here corresponds largely to the shift in ligand π-electron density toward the sodium ion, exceeds $\Delta E_{oi}(\sigma)$ in magnitude in all Na^+ complexes except with N_2. Similarly, $\Delta E_{oi}(\sigma)$ is dominated by the tendency for N-atom lone pair electron donation toward Na^+. Thus both of the major orbital interactions in any given Na^+/ligand complex are, in fact, effects embodied within the ΔE_{ionic} term of our ab initio calculations as presented in Table 3. This observation strengthens our assertion, in section 3.2, that $\Delta E_{orbital}$ from eq 3 is negligible for the Na^+ and K^+ complexes, and we find for these complexes (after considering the difference between the counterpoise-corrected ab initio and the density functional theory BDE values) that generally good agreement is obtained between the ΔE_{ionic} term of eq 3 and the sum $\Delta V_{elst} + \Delta E_{oi}$ of eq 5.

In contrast to Na^+, for Mg^+ the $\Delta E_{oi}(\sigma)$ term (which generally exceeds $\Delta E_{oi}(\pi)$ for these complexes) displays significant variability. For the alkaline earth ion complexes, the ns^1 occupation of the metal ion's valence shell formally permits covalent bonding. The strength of this bonding contribution might be crudely gauged if we assume that the nitrogen atom's tendency for lone-pair electron donation toward the Mg^+ positive charge center is comparable to the corresponding tendency in the Na^+ complex, as encompassed by the consistent Na^+ $\Delta E_{oi}(\sigma)$ values. However, because the optimized M−N distance differs measurably for M = Na versus Mg, it is not ultimately feasible to assign separate covalent and ionic bond strengths to the Mg^+/ligand interaction because of the concerted response of the Pauli repulsion and electrostatic and orbital interaction terms to the metal/ligand separation. Overall, although electrostatic terms dominate the bonding contributions for the Mg^+ complexes in the same manner as that seen for Na^+, the inclusion of covalent interactions within the $\Delta E_{oi}(\sigma)$ term renders invalid for Mg^+ the relation $\Delta E_{ionic} \approx \Delta V_{elst} + \Delta E_{oi}$, which is found to hold tolerably well for Na^+.

Yet larger $\Delta E_{oi}(\sigma)$ terms are seen in the Al^+ complexes, which for Al^+/NC_7H and $Al^+/NC_{2n}N$ (n = 0, 1, 2, 3) have ΔE_{oi} exceeding ΔV_{elst} in magnitude. It is evident that the change in $\Delta E_{oi}(\sigma)$ from Na^+ to Mg^+ to Al^+ is substantially greater than the change in $\Delta E_{oi}(\pi)$ for the same sequence of ions, indicating that the opportunity for covalent bonding in the Mg^+ and Al^+ complexes is a significant factor within the overall BDE of these complexes. The B-LYP calculations also reproduce the finding, seen in Table 1, that the binding energies to cyanopolyynes increase distinctly more steeply with increasing cyanopolyyne size for Al^+ than for Na^+. An increasing covalent interaction between Al^+ and the larger ligands may well account for this difference in Na^+ and Al^+ BDE trends.

We have also performed Morokuma/Ziegler BDE decomposition calculations on the NCCN and HC_3N complexes of Li^+, Be^+, K^+, and Ca^+. These calculations, in concert with the values for Na^+ and Mg^+, allow us to observe that for both the alkali metal and alkaline earth monocations $\Delta E_{oi}(\sigma)$ accounts for a substantially larger fraction of the total BDE for the first-row metal ions than for the second- and third-row ions. Although, as noted above, covalency is not the only factor influencing $\Delta E_{oi}(\sigma)$, the trend described here is consistent with the generally better overlap afforded in covalent interactions involving first-row metal atoms than for those of second- and third-row metal atoms.

3.5. General Discussion and Summary. The metal ion/ligand complexes explored here all feature the coordination of M^+ to the lone pair of an sp-hybridized N atom. The ligand's further structure is effectively totally hidden from M^+ by this eclipsing nitrogen. That the computed M^+/ligand BDE values depend so greatly on the ligand's concealed concatenation of C, N, and/or H atoms thus demonstrates the dramatic influence of the ligand's electron distribution on the M^+/ligand interaction. This influence can readily be rationalized in a qualitative sense by a perusal of the molecular multipole and polarizability tensors displayed in Table 2 or in a more quantitative fashion as discussed in sections 3.2 to 3.4. Nevertheless, it remains notable that for a given metal ion M^+ the optimum distance for σ coordination to N can vary by as much as 0.74 Å, as indicated

in our B3-LYP/6-311+G** optimizations on the Al^+-containing complexes. Thus, although a simple electrostatic model for the M^+/ligand interaction is conceptually very useful in explaining the trend in BDEs, it is clearly inappropriate to view the interaction as a hard-sphere phenomenon. It is also not possible to elucidate a set of effective ionic radii that are consistent with the observed variation in optimized M^+-N distances: whereas for Al^+ this distance contracts by 0.74 Å when HC_5N substitutes for N_2, the analogous contraction for Na^+ is only 0.21 Å. As noted in the preceding sections, the tendency for the more strongly bound alkaline earth ion and Al^+ complexes to exhibit much shorter M^+-N separations than are seen in the weakly bound N_2 complexes of these metal ions is symptomatic of a significant covalent contribution to the bonding between these metal ions and the highly polar cyanopolyyne or polarizable dicyanopolyyne ligands.

How do these BDE values compare with those of other ligands? In recent work,[73] we have used the same levels of theory (CP-dG2thaw and CP-G2) as employed here to determine BDEs for second- and third-row metal ions with NH_3, H_2O, HF, Ne, C_2H_2, and C_2H_4. Our calculated BDEs for σ-coordinated N_2 are only approximately one-half (for alkali metal ions) or one-third (for alkaline earth ions and Al^+) as large as the BDE values for π coordination to either C_2H_2 or C_2H_4. Why then does not N_2, which is formally isoelectronic with HCCH, preferentially adopt π coordination over σ coordination? The quadrupole moment of C_2H_2 encourages π coordination of this ligand, and its polarizability is greatest along the HCCH axis where, however, the locally weak electron cloud in the vicinity of the hydrogen nucleus is an impediment to σ coordination. In contrast, N_2 has a quadrupole moment that directs metal ions toward σ coordination[22] (without any intervening H atoms), and the polarizability, again favoring σ coordination, is considerably smaller overall than for the unsaturated C_2 hydrocarbons. The extreme weakness of the metal ion/N_2 π complex is evident in high-level calculations on the Na^+/N_2 system,[32] which show that this transition structure (to σ-complex N interchange) is stabilized by only about 6 kJ mol^{-1} against N_2 detachment. The Na^+/N_2 π-coordinated geometry thus has a BDE of only ~12% of those values calculated for the analogous C_2H_2 and C_2H_4 π complexes.[47,73]

BDEs for the second- and third-row metal ions with HCN are generally lower than those for NH_3 (only K^+ has a marginally stronger bond to HCN than to ammonia, $BDE(K^+-NH_3) = 72.1$ kJ mol^{-1}),[73] and the difference between NH_3 and HCN BDE values is greater for alkaline earth ions and for Al^+ (e.g., $BDE(Al^+-NH_3) = 134.5$ kJ mol^{-1})[73] than for the alkali metal ions. The strong bonds from NH_3 to those metal ions formally possessing available valence electrons may be a consequence of the greater opportunity for electron sharing when the coordinated ligand possesses a low ionization energy ($IE(NH_3) = 10.07$ eV, cf. $IE(HCN) = 13.6$ eV). Our HCN BDE values are also consistently 3 to 12 kJ mol^{-1} higher than the corresponding H_2O values.[73] In contrast, the high-level calculations that we have undertaken on the NC_4N metal ion complexes yield BDE values consistently lower than the H_2O values, but by at most 8 kJ mol^{-1}. Extrapolation of the trend in dicyanopolyyne binding energies with increasing chain length (Figure 1) makes it apparent that somewhat larger dicyanopolyynes (perhaps NC_8N or $NC_{10}N$) will have metal ion BDEs in excess of those of the water molecule. In this context, it is worth noting also the general similarity between metal ion BDEs for H_2O and for benzene, with η^6 coordination of Na^+ or K^+ to the π^6 electron cloud of C_6H_6 leading to BDEs 10−15 kJ mol^{-1} higher than the corresponding H_2O values obtained through complete basis set limit calculations.[74,75] The calculations reported in the present work demonstrate (so far as we can establish, for the first time) that σ coordination of a metal ion M^+ to a single lone pair on a nonpolar molecule can result in the formation of a metal ion/ligand bond of comparable strength to that ensuing from σ coordination to a highly polar molecule or from π coordination to the delocalized electron cloud of an aromatic molecule such as benzene.

4. Conclusions

High-level quantum chemical calculations reveal several trends in the bond dissociation energies (BDEs) of M^+/ligand complexes where the ligand is an unsaturated, linear N-terminated molecule. Aside from the typical trends expected for such complexes, namely, that BDE values for a given ligand are higher for first- than for second- or third-row metal ions and are higher for alkaline earth monocations than for alkali metal ions and that BDE values for a given metal ion are uniformly lowest for nonpolar N_2 and highest for the largest polar molecule explored here, HC_7N, there are also more subtle tendencies evident. We find that the influence of local bond polarity on the magnitude of the calculated BDE values exceeds that of the molecule's overall polarity (or nonpolarity) because binding energies for the nonpolar larger dicyanopolyynes are seen to converge toward the values exhibited by the largest cyanopolyyne HC_7N. We also find that the alkali metal ion complexes are almost purely ionic in character, whereas significant (although still subservient) covalent character is evident in the alkaline earth ion complexes and in those of Al^+.

Acknowledgment. I thank Rob Dunbar and Eric Magnusson for their insightful perspectives on metal ion complexation and an anonymous referee whose constructive comments have improved the manuscript. This work was supported by the allocation of supercomputing resources, housed at the ANU Supercomputing Facility, from the Australian Partnership of Advanced Computing.

References and Notes

(1) Rodgers, M. T.; Armentrout, P. B. *Int. J. Mass Spectrom.* **1999**, *187*, 359.
(2) Amunugama, R.; Rodgers, M. T. *Int. J. Mass Spectrom.* **2000**, *196*, 439.
(3) Rodgers, M. T.; Stanley, J. R.; Amunugama, R. *J. Am. Chem. Soc.* **2000**, *122*, 10969.
(4) Rodgers, M. T.; Armentrout, P. B. *J. Am. Chem. Soc.* **2000**, *122*, 8548.
(5) Amunugama, R.; Rodgers, M. T. *J. Phys. Chem. A* **2001**, *105*, 9883.
(6) Gapeev, A.; Dunbar, R. C. *J. Am. Chem. Soc.* **2001**, *123*, 8360.
(7) Rodgers, M. T.; Amunugama, R. *J. Phys. Chem. A* **2001**, *105*, 9883.
(8) Rodgers, M. T. *J. Phys. Chem. A* **2001**, *105*, 2374.
(9) Rodgers, M. T. *J. Phys. Chem. A* **2001**, *105*, 8145.
(10) Russo, N.; Toscano, M.; Grand, A. *J. Am. Chem. Soc.* **2001**, *123*, 10272.
(11) El Aribi, H.; Rodriquez, C. F.; Shoeib, T.; Ling, Y.; Hopkinson, A. C.; Siu, K. W. M. *J. Phys. Chem. A* **2002**, *106*, 8798.
(12) Huang, H.; Rodgers, M. T. *J. Phys. Chem. A* **2002**, *106*, 4277.
(13) Rodgers, M. T.; Armentrout, P. B. *J. Am. Chem. Soc.* **2002**, *124*, 2678.
(14) Amunugama, R.; Rodgers, M. T. *Int. J. Mass Spectrom.* **2003**, *227*, 339.
(15) Iceman, C.; Armentrout, P. B. *Int. J. Mass Spectrom.* **2003**, *222*, 329.
(16) Valina, A. B.; Amunugama, R.; Huang, H.; Rodgers, M. T. *J. Phys. Chem. A* **2001**, *105*, 11057.
(17) Elford, M. T.; Milloy, H. B. *Aust. J. Phys.* **1974**, *27*, 211.
(18) Staemmler, V. *Chem. Phys.* **1975**, *7*, 17.
(19) Ikuta, S. *Chem. Phys.* **1985**, *95*, 235.
(20) Pinchuk, V. M. *Zh. Strukt. Khim.* **1985**, *26*, 38.

(21) Dixon, D. A.; Gole, J. L.; Komornicki, A. *J. Phys. Chem.* **1988**, *92*, 1378.
(22) Maitre, P.; Bauschlicher, C. W. *Chem. Phys. Lett.* **1994**, *225*, 467.
(23) Robbins, D. L.; Brock, L. R.; Pilgrim, J. S.; Duncan, M. A. *J. Chem. Phys.* **1995**, *102*, 1481.
(24) Stockigt, D. *Chem. Phys. Lett.* **1996**, *250*, 387.
(25) Tachikawa, H.; Yoshida, H. *THEOCHEM* **1996**, *363*, 263.
(26) Cox, R. M.; Plane, J. M. C. *J. Chem. Soc., Faraday Trans.* **1997**, *93*, 2619.
(27) Falcetta, M. F.; Siska, P. E. *J. Chem. Phys.* **1998**, *109*, 6615.
(28) Jursic, B. S. *THEOCHEM* **1998**, *452*, 203.
(29) Kirschner, K. N.; Ma, B.; Bowen, J. P.; Duncan, M. A. *Chem. Phys. Lett.* **1998**, *295*, 204.
(30) Pullins, S. H.; Reddic, J. E.; France, M. R.; Duncan, M. A. *J. Chem. Phys.* **1998**, *108*, 2725.
(31) Rodriguez-Santiago, L.; Bauschlicher, C. W. *Spectrochim. Acta, Part A* **1999**, *55*, 457.
(32) Soldan, P.; Spirko, V.; Lee, E. P. F.; Wright, T. G. *J. Chem. Phys.* **1999**, *111*, 3420.
(33) Sadlej, J. *Pol. J. Chem.* **1978**, *52*, 2001.
(34) Stockigt, D.; Holthausen, M. C.; Koch, W.; Schwarz, H. *J. Phys. Chem.* **1995**, *99*, 5950.
(35) Petrie, S. *J. Chem. Soc., Faraday Trans.* **1996**, *92*, 1135.
(36) Fitzpatrick, N. J.; Deignan, J. P. *THEOCHEM* **2000**, *505*, 133.
(37) Petrie, S. *Mon. Not. R. Astron. Soc.* **1996**, *282*, 807.
(38) Petrie, S.; Dunbar, R. C. *J. Phys. Chem. A* **2000**, *104*, 4480.
(39) Dunbar, R. C.; Petrie, S. *Astrophys. J.* **2002**, *564*, 792.
(40) Kawaguchi, K.; Kagi, E.; Hirano, T.; Takano, S.; Saito, S. *Astrophys. J.* **1993**, *406*, L39.
(41) Turner, B. E.; Steimle, T. C.; Meerts, L. *Astrophys. J.* **1994**, *426*, L97.
(42) Ziurys, L. M.; Apponi, A. J.; Guelin, M.; Cernicharo, J. *Astrophys. J.* **1995**, *445*, L47.
(43) Ziurys, L. M.; Savage, C.; Highberger, J. L.; Apponi, A. J.; Guelin, M.; Cernicharo, J. *Astrophys. J.* **2002**, *564*, L45.
(44) Petrie, S. *Aust. J. Chem.* **2003**, *56*, 259.
(45) Petrie, S. *Aust. J. Chem.* **2003**, in press.
(46) Petrie, S. *J. Phys. Chem. A* **1998**, *102*, 6138.
(47) Petrie, S. *J. Phys. Chem. A* **2001**, *105*, 9931.
(48) Petrie, S. *J. Phys. Chem. A* **2002**, *106*, 5188.
(49) Becke, A. D. *J. Chem. Phys.* **1993**, *98*, 5648.
(50) Lee, C.; Yang, W.; Parr, R. G. *Phys. Rev. B* **1988**, *37*, 785.
(51) Curtiss, L. A.; Raghavachari, K.; Trucks, G. W.; Pople, J. A. *J. Chem. Phys.* **1991**, *94*, 7221.
(52) Blaudeau, J.-P.; McGrath, M. P.; Curtiss, L. A.; Radom, L. *J. Chem. Phys.* **1997**, *107*, 5016.
(53) Curtiss, L. A.; Raghavachari, K.; Pople, J. A. *J. Chem. Phys.* **1993**, *98*, 1293.
(54) Curtiss, L. A.; Carpenter, J. E.; Raghavachari, K.; Pople, J. A. *J. Chem. Phys.* **1992**, *96*, 9030.
(55) Boys, S. F.; Bernardi, F. *Mol. Phys.* **1970**, *19*, 553.
(56) Siu, F. M.; Ma, N. L.; Tsang, C. W. *J. Chem. Phys.* **2001**, *114*, 7045.
(57) Hofmann, H.; Hansele, E.; Clark, T. *J. Comput. Chem.* **1990**, *11*, 1147.
(58) Duke, B. J.; Radom, L. *J. Chem. Phys.* **1998**, *109*, 3352.
(59) Ma, N. L.; Siu, F. M.; Tsang, C. W. *Chem. Phys. Lett.* **2000**, *322*, 65.
(60) Petrie, S. *J. Phys. Chem. A* **2002**, *106*, 7034.
(61) Frisch, M. J.; Trucks, G. W.; Schlegel, H. B.; Scuseria, G. E.; Robb, M. A.; Cheeseman, J. R.; Zakrzewski, V. G.; Montgomery, J. A., Jr.; Stratmann, R. E.; Burant, J. C.; Dapprich, S.; Millam, J. M.; Daniels, A. D.; Kudin, K. N.; Strain, M. C.; Farkas, O.; Tomasi, J.; Barone, V.; Cossi, M.; Cammi, R.; Mennucci, B.; Pomelli, C.; Adamo, C.; Clifford, S.; Ochterski, J.; Petersson, G. A.; Ayala, P. Y.; Cui, Q.; Morokuma, K.; Malick, D. K.; Rabuck, A. D.; Raghavachari, K.; Foresman, J. B.; Cioslowski, J.; Ortiz, J. V.; Stefanov, B. B.; Liu, G.; Liashenko, A.; Piskorz, P.; Komaromi, I.; Gomperts, R.; Martin, R. L.; Fox, D. J.; Keith, T.; Al-Laham, M. A.; Peng, C. Y.; Nanayakkara, A.; Gonzalez, C.; Challacombe, M.; Gill, P. M. W.; Johnson, B. G.; Chen, W.; Wong, M. W.; Andres, J. L.; Head-Gordon, M.; Replogle, E. S.; Pople, J. A. *Gaussian 98*, revision A.11.3; Gaussian, Inc.: Pittsburgh, PA, 1998.
(62) Becke, A. D. *Phys. Rev. A* **1988**, *38*, 3098.
(63) Baerends, E. J.; A Bérces; Bo, C.; Boerrigter, P. M.; Cavallo, L.; Deng, L.; Dickson, R. M.; Ellis, D. E.; Fan, L.; Fischer, T. H.; Fonseca Guerra, C.; van Gisbergen, S. J. A.; Groeneveld, J. A.; Gritsenko, O. V.; Harris, F. E.; van den Hoek, P.; Jacobsen, H.; van Kessel, G.; Kootstra, F.; van Lenthe, E.; Osinga, V. P.; Philipsen, P. H. T.; Post, D.; Pye, C.; Ravenek, W.; Ros, P.; Schipper, P. R. T.; Schreckenbach, G.; Snijders, J. G.; Sola, M.; Swerhone, D.; te Velde, G.; Vernooijs, P.; Versluis, L.; Visser, O.; van Wezenbeek, E.; Wiesenekker, G.; Wolff, S. K.; Woo, T. K.; Ziegler, T. ADF2002; SCM, Theoretical Chemistry, Vrije Universiteit: Amsterdam, The Netherlands, 2002; http://www.scm.com.
(64) Hoyau, S.; Norrman, K.; McMahon, T. B.; Ohanessian, G. *J. Am. Chem. Soc.* **1999**, *121*, 8864.
(65) McMahon, T. B.; Ohanessian, G. *Chem.—Eur. J.* **2000**, *6*, 2931.
(66) Dunbar, R. C. *J. Phys. Chem. A* **2002**, *106*, 9809.
(67) Morokuma, K. *J. Chem. Phys.* **1971**, *55*, 1236.
(68) Kitaura, K.; Morokuma, K. *Int. J. Quantum Chem.* **1976**, *10*, 325.
(69) Ziegler, T.; Rauk, A. *Inorg. Chem.* **1979**, *18*, 1558.
(70) Ziegler, T.; Rauk, A. *Inorg. Chem.* **1979**, *18*, 1755.
(71) Bickelhaupt, F. M.; Baerends, E. J. In *Reviews in Computational Chemistry*; Lipkowitz, K. B., Boyd, D. B., Eds.; Wiley-VCH: New York, 2000; Vol. 15, p 1.
(72) te Velde, G.; Bickelhaupt, F. M.; Baerends, E. J.; Fonseca Guerra, C.; van Gisbergen, S. J. A.; Snijders, J. G.; Ziegler, T. *J. Comput. Chem.* **2001**, *22*, 931.
(73) Petrie, S. *Int. J. Mass Spectrom.* **2003**, *227*, 33.
(74) Feller, D.; Dixon, D. A.; Nicholas, J. B. *J. Phys. Chem. A* **2000**, *104*, 11414.
(75) Feller, D. *Chem. Phys. Lett.* **2000**, *322*, 543.